



# Experimental assessment of a residential scale renewable–regenerative energy system

A. Bergen, L. Pitt, A. Rowe, P. Wild, N. Djilali\*

*Institute for Integrated Energy Systems and Department of Mechanical Engineering, University of Victoria, Victoria, BC, Canada V8W 3P6*

## ARTICLE INFO

### Article history:

Received 5 July 2008  
Received in revised form  
22 September 2008  
Accepted 22 September 2008  
Available online 7 October 2008

### Keywords:

Hydrogen  
Electrolyser  
Fuel cell  
Regenerative system  
Solar energy  
Transient

## ABSTRACT

An experimental assessment of a hydrogen based regenerative (electrolyser–fuel cell) system is presented. The experiment was conducted on a residential scale Integrated Renewable Energy Experiment (IRENE) test-bed under conditions that are representative of the real demands that would be placed on a solar based, regenerative system, with a focus on dynamic operation under transients in both load and renewable energy supply profiles. A control algorithm employing bus voltage constraints and device current limitations is outlined. Results for a 2 week operating period indicate that the system response is very dynamic but repeatable.

The overall system energy balance reveals that the energy input from the renewable source was sufficient to meet the demand load and generate a net surplus of hydrogen. The energy loss associated with the various system components as well as a breakdown of the unused renewable energy input is presented. In general, the technical challenges associated with hydrogen energy buffering can be overcome, but the round-trip efficiency for the current system is only 22%.

© 2008 Elsevier B.V. All rights reserved.

## 1. Introduction

### 1.1. Scope

As sustainability issues arise with our current energy system, pressure is being applied on policy makers, governments, and the energy sector to provide the energy services we have grown accustomed to with less overall impact on the environment [1]. Renewable resources such as wind, solar and tidal have the potential to supply clean-energy, but their variability poses problems for applications that require a continuous supply of energy.

Energy buffering plays a vital role in enabling transient renewable resources to service user demands. Hydrogen as an energy storage media has potential to address both daily and seasonal buffering requirements. Renewable–regenerative system that employ an electrolyser to convert excess electricity into hydrogen coupled with hydrogen storage and regeneration using a fuel cell (or IC engine) can in principle provide power with zero (or near zero) emissions.

The development of a residential-scale renewable–regenerative system with hydrogen energy buffering was presented in [2]. This paper builds on that prior work and explores the dynamic operation

of the hydrogen energy buffer. Detailed experimental data is presented to (a) expose the operational characteristics of the coupled system, (b) quantify the energy flows within the system, and (c) outline the areas where losses occur. The experimental study was motivated by the need to develop an accurate knowledge of the system response under real operating conditions and to provide experimental data for model validation. Each of the system components has time-dependent characteristics which influence the operation of the combined system. In general, the dynamic aspects of system operation are not adequately considered in the theoretical models of renewable–regenerative systems. Understanding the nature of the interactions and response characteristics for the combined system is essential for designing efficient regenerative systems.

### 1.2. Background

A review of the theoretical models for hydrogen-based renewable–regenerative systems and prior experimental work was given in the previous paper [2]. Several noteworthy additions to the literature have been published in the intervening period.

Modeling efforts have focused on the implementation of hydrogen energy buffering to allow high penetrations of renewable resources into existing power grids [3,4], and the technical feasibility of hydrogen based stand-alone power systems for autonomous mini-grid systems [5–8]. Several models for residential scale

\* Corresponding author. Tel.: +1 250 721 8901; fax: +1 250 721 6323.  
E-mail address: [ndjilali@uvic.ca](mailto:ndjilali@uvic.ca) (N. Djilali).

renewable–regenerative systems have been reported [9–11] that investigate hybrid energy storage systems. A detailed review of individual component models for renewable–regenerative systems is given in [12]. Many of the models discussed in this excellent reference are more sophisticated than those employed in the bulk of the system models described thus far. Finally, issues related to the optimization of control strategies for stand-alone renewable energy systems are addressed by [13,14].

Since the start of the current study, several new renewable–regenerative systems have been or are in development at other research institutes. The HaRI project at West Beacon Farms, Leicestershire, UK, utilizes an assortment of renewable conversion devices, loads and storage technologies as reported in [15]. Two integrated wind-hydrogen renewable energy projects have been developed on remote islands [16,17]. Both are designed as demonstration projects and service a small number of residences (PURE project on Island of Unst, UK, services 5 small business; Utsira on the Island of Haugesund, Norway, supplies 10 households). These projects incorporate hydrogen generation, storage and utilization to buffer the variability of the renewable resource. Common issues reported include underestimation of the wind resource, challenges in system development due to the high number of device interfaces, and regulation/control problems during periods with large power generation and low demand. A fourth system, SYSLAB, incorporating a variety of renewable energy technologies is under development at Riso in Denmark [18]. Experimental work with this platform is focused on control aspects for distributed and decentralized systems.

## 2. Experimental system overview

The Integrated Renewable Energy Experiment (IRENE) test-bed is a residential-scale energy system that employs regenerative components (electrolyser and fuel cell) to enable intermittent energy sources to service time-varying loads. During the system conceptual design stage, sizing issues were considered, taking into account a range of practical constraints including: project budget, available laboratory space, size and capacity of relevant commercial components (renewable energy converter, fuel cells, electrolysers, inverters etc.), and the scale of systems typically modeled in the literature. The outcome was the selection of a target system capacity in the 3–4 kW range. This capacity is similar to the typical electric demand of a Canadian residence [19]. The basic IRENE system schematic is presented in Fig. 1 and a summary of the primary system components is listed in Table 1.

A detailed description of the IRENE system is given in [2]. A brief overview to provide context for the current work follows. Energy fluxes, measured in real time (or time series from other sites), are

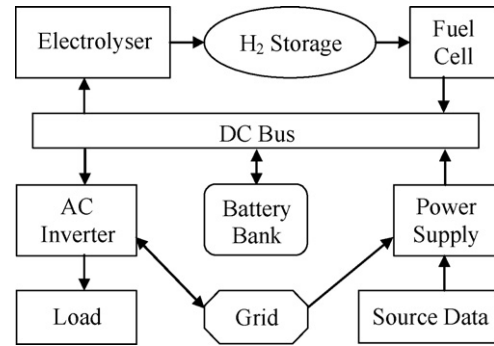


Fig. 1. IRENE test platform schematic.

processed by suitable transfer functions representing a renewable energy conversion device (i.e., wind turbine, solar array, microhydro plant). The output is used to control a 15 kW Lambda EMI ESS programmable power supply which provides power to IRENE's common 48 V DC bus. A 4 kW Xantrex inverter supplies AC power from the bus to the load. The output hardware is configured to support real loads (induction motors, switching loads, etc.) as well as a 3 kW NHR programmable load bank that can simulate a residential load profile.

During periods in which the input power exceeds the demands, excess electrical energy is converted to hydrogen via a 6 kW Stuart Energy electrolyser. IRENE is outfitted with metal hydride and gaseous (10 and 200 bar) hydrogen storage systems. A 1.2 kW Ballard Nexa fuel cell is employed to convert stored hydrogen to electricity during periods of insufficient renewable input. Interfacing the fuel cell into the DC bus was accomplished by floating the fuel cell on a secondary power supply which increases the apparent output from the 'fuel cell system' to approximately 2 kW. A small 272 Ahr battery bank maintains bus stability under transient loads but is not sized for primary energy storage.

The test-bed is fully instrumented to measure energy and mass flows between system components. An integrated PC-based control system allows for long-term operation of the system following a user specified control algorithm.

A primary motivation for developing the IRENE test-bed was to create a platform for examining the operating characteristics of a renewable–regenerative system in a controlled environment. The goal was to observe the dynamic response and interplay between components as the system responds to the demands of a time varying load and resource input. To this end, an experimental investigation coupling all of the IRENE sub-systems was undertaken. The results from this multi-week experiment are presented fol-

Table 1  
Summary of primary system components.

	Manufacturer/type	Maximum current (A)	Potential (V)	Power (W)
Bus	n/a	>250	42–56 48 nominal	n/a
Fuel cell	Ballard Nexa PEM	0–45	46 V at 0 A 22 V at 45 A	1,200
Electrolyzer	Stuart Energy SRA	107	42–56	6,000
Battery	GNC Absolyte IIP deep cycle AGM	272 A h	42–56 48 nominal	
DC power supply	Lambda EMI ESS	250	0–60	15,000
Load	NHR model 4600	27	110 VAC	3,000
Inverter	Xantrex SW4840	180 peak for short duration	44–62 48 nominal	4,000

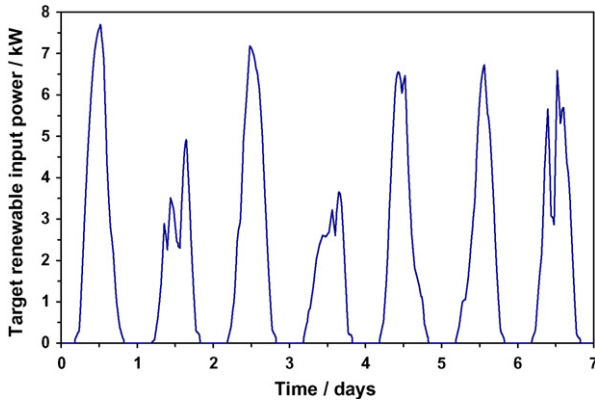


Fig. 2. Solar resource input profile.

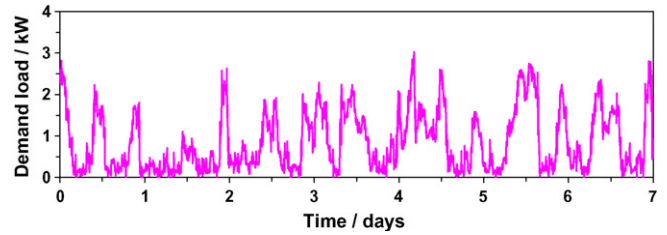


Fig. 3. Demand load profile.

lowing a description of the resource, load, and control algorithm implemented.

### 3. Resource and load profile definition

The resource data employed in the experiment was obtained from Natural Resources Canada for a solar-based renewable power system [20]. The data was previously used in a simulation study conducted in “RE-H2” a modeling program developed by NRCan to investigate hydrogen and renewable energy applications in residential buildings. The profile was calculated for a residential scale system, in summer time operation near Ottawa, Canada, based on local insolation data, PV module performance specifications, array size, orientation, etc. The data was available as a 7 day time series with 5 min resolution, illustrated in Fig. 2.

The daily power profile reflects the natural variability of a solar resource. Scaling of the profile was not required since the peak magnitude (7.7 kW) was within the working range of IRENE and was reasonable considering the nominal power rating of the load bank and electrolyser (3 and 6 kW respectively).

The demand load, illustrated in Fig. 3, is derived from measured load data for typical British Columbia residences, courtesy of BC Hydro [21]. The data is from single family dwellings, taken at a similar time of year (July 3–9) as the solar resource data. The peak load is limited to 3 kW to fit the capacity of the programmable load bank.

During the course of the experiment, the 7 day resource and load pattern is repeated multiple times so that changes in performance are detectable. Thus, the stability of the system can be assessed.

Since the hardware responds to the input and demand profiles in real time, a control algorithm is required to guide system operation.

### 4. Control methodology

IRENE is a complex system and requires a dedicated controller to supervise equipment operation during a long-term experiment. A detailed description of the specific control algorithm is beyond the scope of the current work. However, some knowledge of the control methodology is required to provide a framework for subsequent discussion of the system.

The IRENE system controller is implemented within the main data acquisition program and therefore has direct access to all measured system parameters (voltages, currents, flow rates, temperatures, etc). The IRENE system controller manipulates the set-points of the renewable input power supply, fuel cell system, electrolyser stack current control module, and AC load bank (see Fig. 4) to achieve the control objectives outlined in Fig. 5.

The primary controller objective is to apply the specified renewable input power profile and demand load while directing power transfer between system components (control statement 1). To accomplish this, the bus voltage must remain within a range that maximizes the controller’s ability to distribute power. Since the electrolyser power consumption is manipulated through passive reduction of the input voltage, the broadest range of control options exist at high bus voltages. Thus, the system controller attempts to maintain the bus voltage at 54 V which corresponds to the battery float voltage (voltage at 100% state-of-charge) and the maximum sustained electrolyser input voltage. The maximum allowable bus voltage is 56 V based on battery, Nexa filter module, and electrolyser input voltage constraints. Momentary operation above the target 54 V bus voltage occurs while the controller responds to changes in the load and input power settings. However, prolonged operation at bus voltages exceeding 54 V (control statement 2) will result in permanent battery damage and therefore must be avoided.

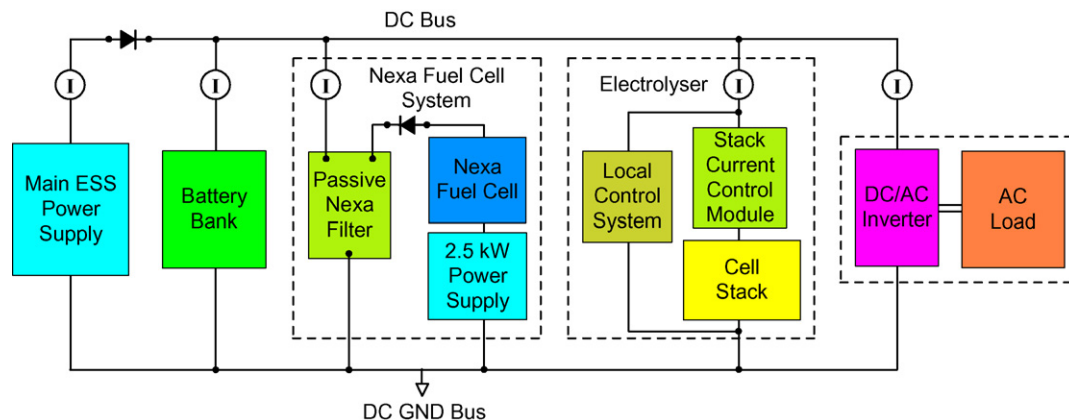


Fig. 4. Multi-week experiment hardware configuration.

<p>1) Primary control objectives:          apply renewable input power as per data file value          apply AC load demand as per data file value          maintain <math>V_{\text{bus}} = V_{\text{bus target}} = 54 \text{ V}</math> while using all available renewable input power</p> <p>2) Control action for excess renewable input:          If <math>V_{\text{bus}} &gt; 54 \text{ V}</math> then:          limit renewable input power</p> <p>3) Battery current constraint:  <math>-35 &lt; I_{\text{battery}} &lt; 17 \text{ A}</math> (supplement renewable input power if required)</p> <p>4) Electrolyser operating condition:  <math>I_{\text{bus excess}} \geq I_{\text{elect min threshold}} = 13 \text{ A}</math></p> <p>5) Fuel cell operating condition:          If <math>V_{\text{bus}} &lt; V_{\text{fuel cell engage threshold}} = 48 \text{ V}</math> then:          operate fuel cell so <math>0 &lt; I_{\text{battery}} &lt; 5 \text{ A}</math> up to <math>P_{\text{max fuel cell}}</math></p> <p>6) Hydrogen buffer operation constraint:          fuel cell and electrolyser operation is mutually exclusive</p> <p>7) Low bus voltage condition:          If <math>V_{\text{bus}} &lt; V_{\text{low bus shutdown threshold}} = 46 \text{ V}</math> then:          supplement input renewable input power</p>
---

Fig. 5. IRENE control logic statements and constraints.

#### 4.1. Control – excess renewable input

When the renewable input power exceeds the AC load demand, the IRENE system controller assesses the battery state-of-charge (SOC) to determine if the energy should be directed to temporary storage or hydrogen production. Maintaining a high battery SOC has priority over hydrogen production. However, battery charge rate limitations (control statement 3) may dictate that the power be split between the two energy sinks. The electrolyser is operated when the IRENE system controller detects that sufficient ‘excess’ power exists to meet the minimum electrolyser threshold input current (control statement 4). The current set-point of the electrolyser stack current control module is adjusted to track the excess power.

At any instant, the system may not be able to consume all of the available renewable input power due to device limitations and dynamic response rates. The difference between the available renewable input power (i.e., the data file value) and the actual power delivered to the system is defined as the ‘unused’ renewable input power. Since the available renewable input power is a construct within the control system (i.e., a number from a data file) the ‘unused’ designation refers to power was never introduced to the IRENE system. All real power delivered to the IRENE bus by the power supply or fuel cell system is distributed to the various loads or energy buffers.

Assuming the electrolyser is sized properly, renewable input power may remain unused for three reasons. First, if the excess is insufficient to meet the electrolyser’s minimum input requirement, then the surplus is effectively lost. Second, the excess power is within the electrolyser’s nominal working range but is not absorbed due to dynamic response limitations. Details of the electrolyser’s transient response are discussed in [22]. Third, power may remain unused due to limitations in the control system’s ability to track the renewable input and distribute power. Losses are primarily due to controller dead-band combined with the hardware limitations

of the electrolyser current control module, outlined in [2,23]. In post-experiment analysis, the ratio of the unused renewable input relative to the available renewable input is an important measure to assess overall system performance.

#### 4.2. Control – excess demand loads

In operating scenarios where the load demand exceeds the renewable input, the power balance must be met by the energy buffer. The battery bank is the primary resource for servicing short-term imbalances. Once the batteries are depleted to an intermediate SOC, the fuel cell is invoked. Since the actual battery demands were unknown before conducting the experiment, a maximum battery discharge current (control statement 3) was established as a safeguard. If the discharge current exceeds the 35 A limit, the IRENE system controller temporarily increases the main power supply power setting to lower the battery discharge current to the specified limit value.

Bus voltage is used as an indicator of battery SOC. Advanced integration schemes exist to monitor SOC but require in-depth battery characterization and are sensitive to minor changes in long-term battery performance [24]. Although voltage does not predict battery SOC with great precision, it is sufficient for this application. In the IRENE system the working voltage range of the bus is 54–46 V.

The fuel cell power contribution is moderated to provide a net positive battery current when the bus voltage is below the 48 V fuel cell engagement threshold (control statement 5). This threshold was chosen to ensure that a minimum residual battery capacity is available to buffer the fuel cell output. The control method employed restricts fuel cell operation to servicing the imbalance between the renewable input power and the demand load. Thus, the fuel cell is not used to recharge the batteries except in cases where the battery voltage has dropped below the fuel cell engagement threshold voltage due to excess load. When the net imbalance is reduced to a level within the fuel cell power output range, the batteries are gradually recharged until the bus reaches the fuel cell engagement threshold voltage.

Fuel cell and electrolyser operation are mutually exclusive (control statement 6). Clearly generating hydrogen based on fuel cell derived power is counter productive from an energy standpoint due to the losses involved (i.e., it is irrational to use a given amount of hydrogen to make less hydrogen).

An additional feature has been incorporated to prevent battery discharge beyond the recommended minimum SOC. If the bus voltage drops below the low bus shutdown threshold voltage (control statement 7), the main power supply is adjusted to provide a net zero battery current. By intervening in this manner, premature termination of the experiment due to low voltage shutdown of the inverters (a hardware safety feature) is avoided. Application of the low bus voltage safety system constitutes a ‘failed’ experiment from an energy balance perspective. However, it allows a measure of freedom to explore load profiles that push the system to the limit. The power artificially added due to battery current limiting and the low bus safety system is recorded for post-experiment analysis. The ratio of the energy added to maintain the control objectives to the actual input energy provides another metric for assessing system performance.

## 5. Experimental results

A multi-week experiment was conducted based on the resource and load profiles specified in Section 3 and the control methodology outlined in Section 4. Throughout the experiment, currents, voltages, temperatures, flow rates, etc., were sampled on a continuous basis at roughly 10 kHz. Average values for all parameters were



logged on 6 s intervals resulting in some 4 million recorded data points for the 2 week period under investigation.

Based on the measurements taken, the total energy input to the system from the renewable input proxy, batteries, and fuel cell system during the 14 day experiment is 726.7 kWh. Likewise, the total energy consumed by all energy sinks is 728.0 kWh. The difference, 1.3 kWh or 0.2%, represents the net error associated with the measurement devices, calibration constants, and losses in precision due to truncation of data in the recording process. The error is negligible and indicates that data can be reported with a high degree of confidence.

### 5.1. Bus voltage response

Bus voltage is a key system parameter since it influences the power transfer that can occur between components. A plot of the bus voltage over the 2 week experiment is given in Fig. 6. Data is grouped into 1 week segments and arranged to allow comparisons between similar days in the operating cycle. The target renewable input power and load profiles are included for reference (plots 6-A and 6-B). The high degree of similarity in bus voltage between

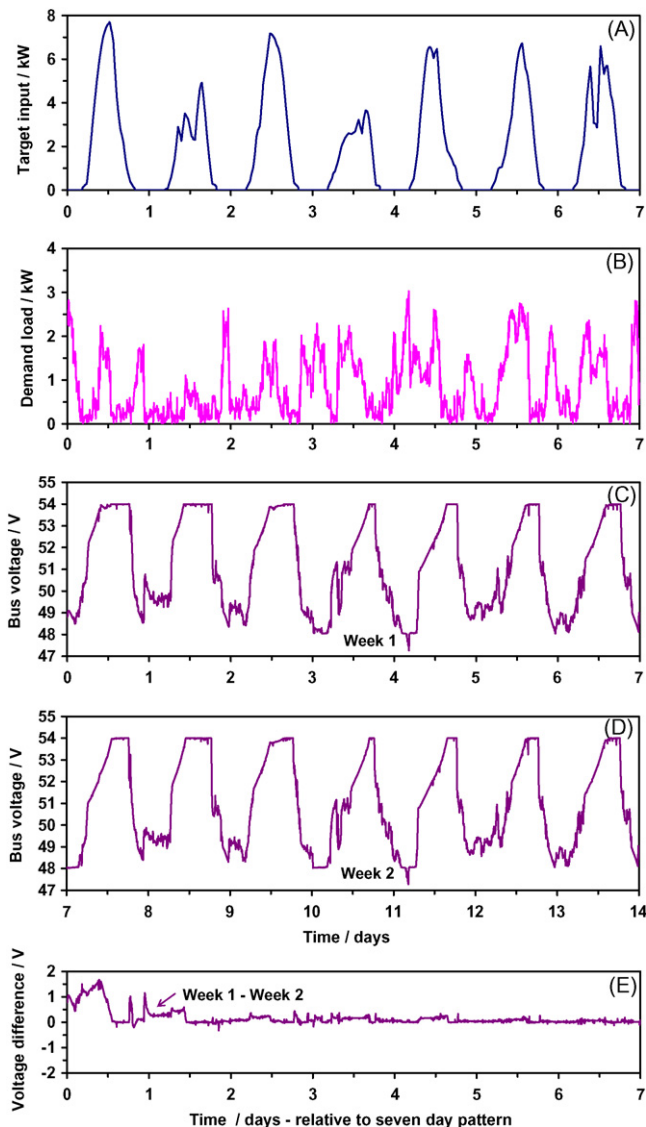


Fig. 6. Basic system response.

weeks 1 (plot 6-C) and 2 (plot 6-D) indicates that the system is responding in a consistent manner. The net difference in bus voltage for similar time periods is compared in plot 6-E. After day 2, the voltage difference is, on average, less than 0.2 V. The largest difference occurs between days 1 and 8, but even this is less than 2 V.

The experiment begins with a period of zero renewable input power and high load demand. Although the batteries are fully charged at the start of day 1 (i.e.,  $V_{\text{bus}} = 54 \text{ V}$ ,  $I_{\text{battery}} = 1 \text{ A}$  to maintain the float voltage), the high initial battery discharge immediately lowers the effective bus voltage to 49 V. This illustrates the dynamic range in bus voltage that occurs due to the limited battery buffering capacity. Daily bus voltage swings ranging from 5 to 6 V are noted. The small differences noted above between days 1 and 8 are associated with the initial transition to a stable operating cycle, which occurs in conjunction with the high initial SOC and rate of discharge of the battery during day 1, and with the electrolyser transition losses which are higher than day 8 because the electrolyser operates for a larger portion of the day in thermal limiting mode.

The bus voltage achieves the target operating voltage of 54 V for a minimum of 3 h each day. This does not imply that the batteries are fully charged, but rather that battery charge rate limiting is not in effect during those intervals. Results from other experiments have shown that the batteries require approximately 24 h at 54 V to reach full charge. The need for active limiting of the bus voltage at the target voltage is evident given the duration of each day that is spent at the upper bound. Serious battery damage would occur due to an over voltage condition if the bus voltage was left unconstrained.

Periods during which the bus voltage is held constant at 48 V indicate times when the fuel cell's output capacity is sufficient to meet the load. Day 4 has the lowest net renewable input energy of the 7 day pattern and battery recharging is limited by the brief period that the bus is maintained at 54 V, less than 3 h. By the early part of day 5, the battery buffer is depleted and the fuel cell is required to service the load. During this period, the bus voltage drops below the 48 V fuel cell threshold voltage indicating that the fuel cell is unable to supply sufficient power to meet the demands. The overload condition lasts approximately 20 min, but within an hour, the bus voltage has been resorted. This event illustrates that the control methodology developed for the system is robust enough to handle real operating demands. Throughout the experiment, the bus voltage remained above the critical low level threshold so intervention by the low bus safety system was not required.

Given the consistent bus voltage response, subsequent time series plots will be presented for the second week of data only.

### 5.2. Input energy details

Input power transfer to the IRENE DC bus is managed by the IRENE system controller which attempts to apply the target renewable input profile defined in the data file. Control bounds identified in Section 4 may necessitate that the actual power supplied deviate slightly from the target to ensure that operational constraints are met. A detailed breakdown of the input to the system for week 2 is given in Fig. 7. Note that the scales of the various subplots are individually scaled to maximize vertical resolution.

Plot 7-A is the target (ideal) 7 day input power profile from the renewable source. The ideal input energy, 626.3 kWh, for the 2 week experiment can be obtained through the appropriate integration calculations. A summary of the energy calculation for all key parameters is reported in Table 2 for the 2 week period.

The actual input profile supplied by the IRENE power supply (renewable input proxy) is illustrated in plot 7-B. The energy content is 602.4 kWh. Of this, 10.1 kWh is artificially added by the system controller (see plot 7-C) to limit the battery discharge rate

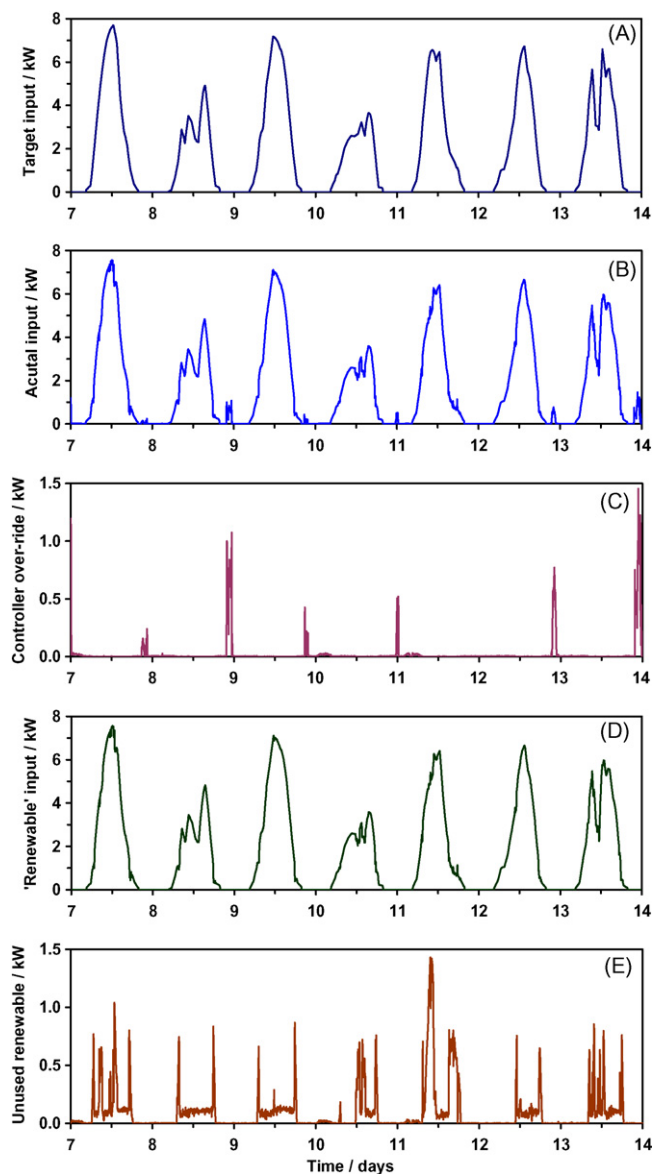


Fig. 7. Week 2 input power breakdown.

Table 2

Energy balance summary for the 2 week experiment.

	Days 1–14 (kWh)
Target renewable input energy (A)	626.3
Energy supplied by renewable power supply proxy	602.4
Portion artificially added by control system	10.1
Portion associated with 'renewable' resource (B)	592.3
Energy supplied by fuel cell	19.2
Hydrogen consumed	14.7 (m <sup>3</sup> )
Energy supplied by batteries	105.1
Energy source sub-total	726.7
Energy input to batteries	107.6
Energy input to inverter	314.9
Energy delivered to AC load	290.7
Energy diverted to electrolyser	305.5
Energy input to electrolyser stack	283.6
Hydrogen produced (m <sup>3</sup> )	51.9 (m <sup>3</sup> )
Energy sink sub-total	728.0
Total unused renewable input (A–B)	34.0
Portion due to minimum electrolyser input threshold	14.0
Portion due to electrolyser transition rate limitations	10.6
Portion due to tracking and distribution limitations	9.4

as per the control objectives outlined in Section 4.2. The added power occurs during periods with no renewable input energy. The energy added is only 1.5% of the actual input energy. This indicates that energy buffering capacity is generally sufficient to meet the load demands during periods with low renewable input given the specific load and resource profiles. It is feasible that the energy supplement could be reduced to zero by increasing the battery discharge current limit as it was set at a rather conservative level, only 35 A.

The energy input to the system associated with the 'renewable' source can be obtained by subtracting the power artificially supplied (plot 7-C) from the actual input power (plot 7-B). The result is illustrated in plot 7-D. The profile closely resembles the target input but contains some higher frequency artifacts introduced by the control system. The associated energy content is 592.3 kWh.

The unused renewable input is defined as the difference between the target input and the 'renewable' input profile as illustrated in plot 7-E. The total unused renewable input energy is 34.0 kWh or 5.4% of the ideal renewable input. Substantial variation in the daily unused renewable energy occurs, with daily variations ranging from a low of 2.7% to a high of 10.7%, indicating that system performance is dependent on correlation between the input and load profiles. On all days, sufficient unused renewable input energy is available to offset the energy added by the IRENE system controller to meet the specific control constraints. A detailed breakdown of the unused renewable energy is presented in Section 5.4.

### 5.3. Energy transfer details

The power transfer among system components follows the profiles outlined in Fig. 8. The actual input power profile (plot 8-A) and bus voltage (plot 8-B) are repeated for reference.

#### 5.3.1. Output load serviced

The entire 290.7 kWh AC demand load is serviced by the renewable input and energy buffer sub-systems. The input energy to the DC/AC inverter is 314.9 kWh, resulting in a 92.3% average conversion efficiency between the DC bus and the AC load.

#### 5.3.2. Battery contribution

The power delivered to the system bus by the batteries is illustrated in plot 8-D. Positive values indicated power delivered to the bus by the batteries while negative values denote power supplied by the bus for battery recharging.

At the start of the experiment, the batteries were fully charged. Over the 2 week period, the batteries contributed a total of 105.1 kWh to the bus. Conversely, they absorb 107.6 kWh for recharging. Batteries require more energy to recharge than what is released during discharge due to the internal losses involved [24]. The estimated final battery SOC is 30%. While the total battery energy transfer values are important for evaluating the system energy balance, they are not appropriate for calculating the battery round-trip efficiency because of the different initial and final SOC.

The decrease in battery SOC is explained as follows. An initial ramp in period is required for the system to achieve repeatable performance. The bus voltage on the first day was on average higher than day 8, so a larger proportion of the renewable input was directed to hydrogen production while the batteries supplied the AC output load. During the final 5 h of day 14, the batteries were supplying energy to the load and were thus being depleted. Therefore the battery SOC at the end of the experiment should be lower than at the start given the additional discharge involved.

A clearly defined recharging pattern is evident consisting of a period of relatively constant power draw at approximately  $-1$  kW

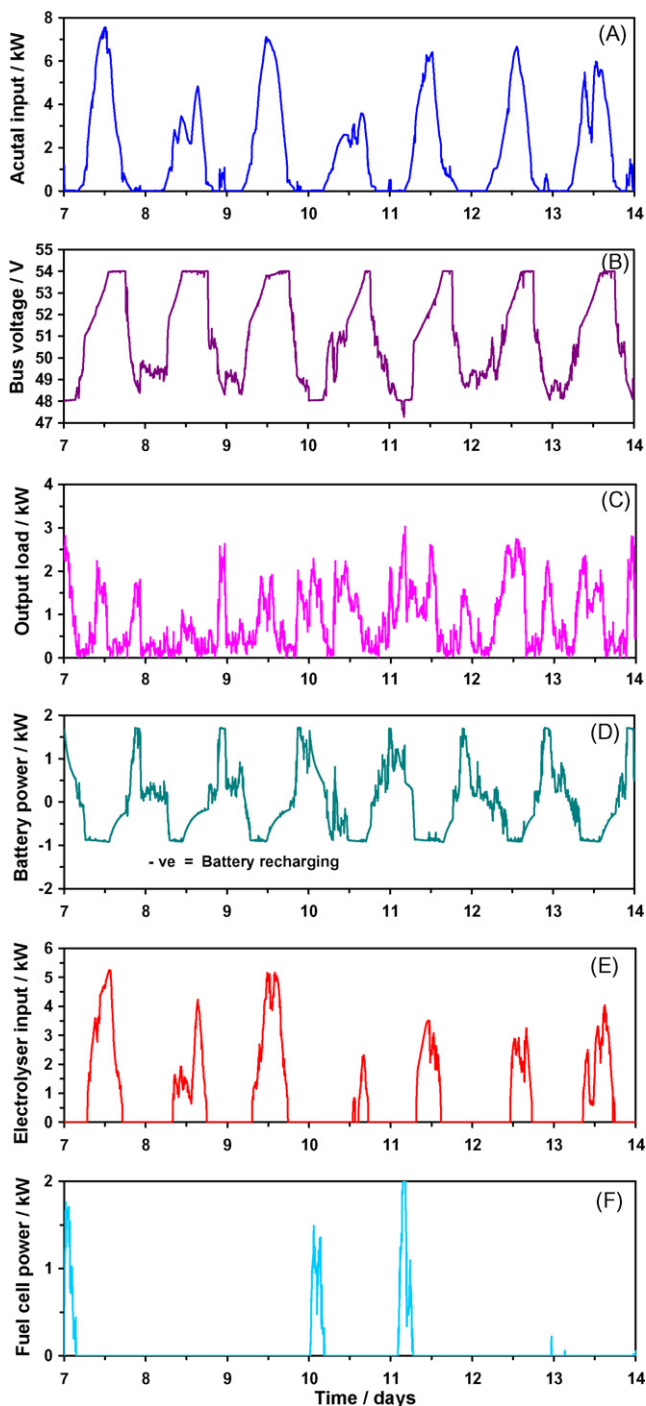


Fig. 8. Week 2 power transfer breakdown.

(i.e., recharging at the limiting current value) followed by a gradual decay in power absorbed during constant voltage recharging (i.e., once the bus reaches 54 V). The relative smoothness of the recharging profile compared with the discharge portion indicates that the IRENE system controller is able to maintain the specified battery charge limiting conditions. Conversely, it implies that during the battery recharge period, the electrolyser is absorbing the difference between the renewable input and the load demands.

The pattern of battery energy supply/draw during the experiment is more important than the specific final SOC value. After

the first 2 days, a consistent pattern of energy flow to and from the battery buffer is established indicating that the experiment is not depleting the batteries' temporary energy store to supply a net system energy imbalance. If five 7 day periods between days 3–10 and days 7–14 are investigated, the batteries contribute on average a total of  $51.4 \pm 0.2$  kWh to the bus and absorb  $55.9 \pm 0.3$  kWh for recharging giving a nominal 91.9% round-trip efficiency.

In the IRENE system, the batteries are required to buffer currents at the Hz level (predominately 120 Hz) due to the demands of the AC inverters. The time series plot suggests that they also play an integral buffering role at the minute to hourly level given the 'high frequency' signal content when plotted on a daily time scale. Based on the 7 day intervals used to evaluate the battery round-trip efficiency, the batteries supply 32.7% of the energy delivered to the inverter to service the output load.

### 5.3.3. Hydrogen production

Surplus renewable input energy was available each day for electrolyser operation as illustrated in plot 8-E. Days 9 and 14 clearly demonstrate the unsteady nature of the input power profile that an electrolyser is subjected to under real system operating conditions. The profile has little in common with the steady-state test conditions typically used in electrolyser characterization work.

In total, the IRENE system controller diverted 305.5 kWh to the electrolyser, which ran for 114.5 h. Therefore, 51.6% of the 'renewable' input energy is transferred to the hydrogen buffer. The electrolyser stack consumed 283.6 kWh for a net electrolyser input utilization ratio of 92.5%. The electrolyser's local control system and ancillary devices consumed 4.1 kWh of the input energy and the balance was dissipated by the stack current control module. Hydrogen compression was not performed during the experiment due to equipment limitations. Compression is an energy intensive process and would add a substantial parasitic load to the electrolyser system (approximately 1/5 of the total input energy).

The net hydrogen output from the electrolyser is  $51.9 \text{ m}^3$  at STP. Based on the higher heating value ( $141,780 \text{ kJ kg}^{-1}$  [25]), the energy content of the hydrogen is 183.8 kWh resulting in an electrolyser energy efficiency of 60.2%. Daily efficiencies vary by  $\pm 5\%$ .

### 5.3.4. Hydrogen consumption

The fuel cell was required to supply power to the DC bus three times during the week as shown in plot 8-F. In total it operated for 21 h and contributed 19.2 kWh to the bus. This represents 6.1% of the energy delivered to the inverter to service the output load. The fuel cell consumed  $14.7 \text{ m}^3$  of hydrogen at STP, which is equivalent to 28.3% of the hydrogen generated by electrolysis of the excess renewable input. Based on the higher heating value of the hydrogen consumed, the average fuel cell energy efficiency is 36.8%.

By the end of the experiment,  $37.2 \text{ m}^3$  of surplus hydrogen existed. Given the fuel cell's hydrogen consumption to net energy output, a projection of the fuel cell output for the full  $51.9 \text{ m}^3$  of hydrogen generated is 67.8 kWh. In this case, a hydrogen energy buffer efficiency of 22.2% would be realized.

Table 3 provides a summary of the energy inputs/outputs and efficiencies.

## 5.4. Unused energy details

In the IRENE system, any excess energy should, in principle, be converted into hydrogen by the electrolyser. In reality, the electrolyser is unable to utilize all of the available excess renewable input energy as illustrated in Fig. 9. The electrolyser input power, plot 9-A, is included to reference the basic operating periods. Plot 9-B is the total unused renewable input energy as defined in Section 5.2.



**Table 3**  
Main energy transfers and efficiencies.

	Energy (kWh)	%Efficiency
Renewable source total input to system, $E_{\text{ren}}$	592.3	
Renewable energy input to electrolyser, $E_{\text{in}}$	305.5	
Electrolyser control and ancillaries	21.9	
Net input to electrolyser stack	283.6	
Hydrogen produced, $E_{\text{H}_2}$ ; $\eta_{\text{electrolyser}} = E_{\text{H}_2}/E_{\text{in}}$	183.8	60.2
Fuel cell output, $E_{\text{FC}}$ ; $\eta_{\text{FC}} = E_{\text{FC}}/E_{\text{H}_2}$	67.8	36.8
Round trip efficiency; $\eta_{\text{RT}} = E_{\text{FC}}/E_{\text{in}}$		22.2

\* Fuel cell output extrapolated from 21 h of operation.

#### 5.4.1. Electrolyser minimum input limitations

Losses occur prior to electrolyser start-up or following shut-down when the excess power is insufficient to meet the electrolyser's minimum operating requirement, as shown in plot 9-C. They account for 14.0 kWh or 41.2% of the total unused renewable input. The quantity of power lost due to the minimum threshold is influenced by a combination of factors including the renewable input power profile, load demands, and battery recharge requirements. Two general classes of days are observed.

On days with a strong renewable input and moderate loads, day 10 for instance, only a small portion of the excess power is lost

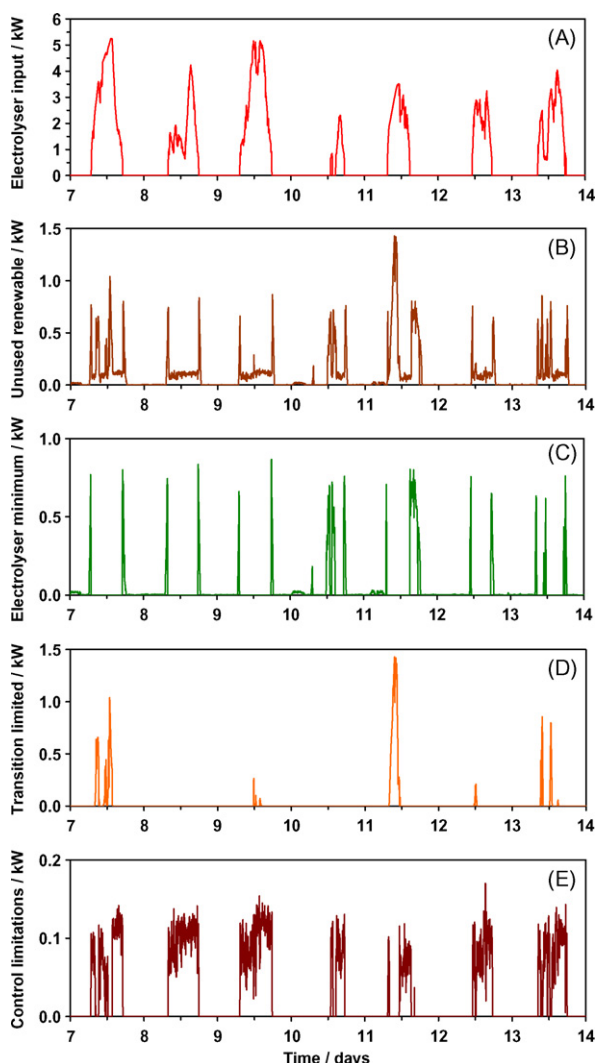


**Fig. 9.** Week 2 unused renewable input breakdown.

due to the minimum electrolyser requirement. In comparison, on a day where the renewable input is barely sufficient to meet the load demand, for example day 11, significant power is lost since the excess fails to meet the electrolyser minimum during a large portion of the day. The energy lost due to the minimum electrolyser input on day 11 is over 3 times that of day 10.

#### 5.4.2. Electrolyser transition rate limitations

The unused renewable input due to the electrolyser's dynamic response is illustrated in plot 9-D. In this case, the electrolyser power draw is limited by the transition rate characteristics and therefore is unable to absorb all of the available excess power. This phenomena accounts for 10.6 kWh or 31.2% of the total unused renewable energy.

Losses due to the electrolyser's thermal transition are most pronounced on days where surplus power is available but substantial battery recharging required, for instance day 12. In this case, the bus voltage and hence the electrolyser input voltage is limited by the battery recharge rate. The voltage constraint reduces the rate at which the electrolyser reaches operating temperature. During the warm-up period, the effective input power capacity is lowered and the electrolyser may be unable to make full use of the excess renewable input.

On a per event basis, the unused energy associated with the electrolyser transition limit is typically larger than for the minimum electrolyser threshold but occur less frequently.

#### 5.4.3. Power tracking and control limitations

The unused renewable energy associated with the control system's limitations on identifying and diverting the 'excess' power to the electrolyser is illustrated in plot 9-E. The losses are directly correlated with the electrolyser's operating duty cycle and are relatively constant at 100 W. During the 2 week experiment, 9.4 kWh or 27.6% of the available excess renewable input remains unused due to this limitation. This is equivalent to 1.6% of the total renewable input.

In the existing control system, a balance between the dead-band required for control stability and the power transfer to the hydrogen energy buffer was established. Potential exists to improve the renewable resource utilization by implementing an advanced system controller. However, careful attention must be paid to maintaining control stability under dynamic operation conditions.

## 6. Discussion

The overall system energy balance indicates that the energy input from the renewable source was sufficient to meet the demand load. Furthermore, the energy buffer system was able to capture a significant portion of the daily excess energy and store it as hydrogen. The time series plots illustrate that the system response is highly dynamic but generally repeatable.

Operational experience gathered with the IRENE system indicates that the short-term energy buffer, the battery bank in this case, plays an important role in maintaining system stability. The IRENE system was designed with an emphasis on hydrogen as the primary energy buffer. As a result, the battery capacity was intentionally minimized. However, the actual current flows observed on the 'DC' bus more closely resemble that of an AC system due to the output inversion demands. Large variations in bus voltage occur over the course of each day due to the low overall battery capacity. Therefore, buffering for medium time scales (minutes and hours), short time scales (120 Hz fundamental) and high frequency (kHz range) events must not be underestimated in systems that employ hydrogen technologies for energy buffering. The relative importance of this fact was not evident at the onset of the project but



was emphasized during actual system operation. Renewable energy systems with minimal short-term energy buffering will require robust system components to handle the extremes in bus voltage swings.

The battery power and bus voltage profiles indicate that the IRENE system controller was able to maintain the control objectives by proportioning the power diverted to the batteries and the electrolyser. However, to accomplish this with a real input and load profile, the electrolyser is subjected to an input power profile with considerable high frequency content. Experimental results conducted with the IRENE system (presented in a companion paper [22]) indicate that the electrolyser performance can be compromised under dynamic loading conditions. While the electrolyser can tolerate a wide variation in input power, the system must have sufficient short-term energy buffering capacity to maintain the minimum demands of the electrolyser as well as the other system loads. If the system is unable to support the combined load, experiments have shown that shutting the electrolyser off for a minimum rest period, may in fact, lead to improved overall system performance in comparison to continued start/stop operation. In light of these findings and the system response demonstrated herein, a comprehensive understanding of the electrolyser's dynamic response is required for accurate modeling of renewable–regenerative systems and development of control strategies.

## 7. Conclusions

A multi-week experiment was conducted to determine the response of the IRENE system to operating conditions that are representative of the real demands that would be placed on a solar based renewable–regenerative system.

On an energy basis, the IRENE system was able to directly service the load given the input energy available from the renewable resource. However, on average, 5.4% of the available renewable input energy remains unused due to system limitations. Energy lost due to the electrolyser minimum operating conditions accounts for 41% of the unused renewable input energy while the electrolyser transient response accounts for 29%. The balance is due to control system limitations in tracking and distributing the surplus renewable power.

The batteries play an important role in maintaining the daily energy flows buffering approximately 1/3 of the output demand. But over the long term, the system does not deplete the batteries' energy store to make up for net deficiencies in the renewable input (i.e., the system is operating in a sustainable manner). Roughly 1/2 of the renewable input energy is directed to hydrogen production and converted with 60% energy efficiency. The fuel cell consumes approximately 1/4 of the hydrogen produced to offset 6% of the demand load during periods with low renewable input, resulting in a net surplus of hydrogen at the end of the 2 week period.

From an overall energy stand point, the experiment is a success. However, the projected round-trip efficiency of the hydrogen energy buffer (based on total fuel usage) is only 22% versus 92% for the battery buffer.

The present experiments were conducted using profiles of demand loads and solar resource profiles that are representative but specific to a region (British Columbia) and season (summer).

The data should be valuable to guide and help validate dynamic model developments. Clearly, it would be instructive to perform an analysis of the system performance using a range of load and supply scenarios. Nonetheless a number of conclusions drawn from this study are expected to be broadly informative. The energy penalty associated with the technology cannot be overlooked when evaluating the potential of hydrogen against other energy buffering techniques. In certain applications, such as remote locations where alternate energy services are not available, the losses associated with the energy buffer may be acceptable. However, when other energy sources exist, it may be more effective and expedient to directly utilize the renewable source when it is available, and employ an alternate form when it is not. In either case, the operation of the IRENE system illustrates that if the ratio between the renewable input and demand load falls within the prescribed bounds it is technically possible to service user demand load by employing hydrogen energy buffering. The actual viability of such systems would ultimately be determined by economic and environmental considerations outside the scope of this work.

## Acknowledgement

This work was funded by Natural Resources Canada and Western Economic Diversification Canada.

## References

- [1] G. Boyle (Ed.), *Renewable Energy: Power for a Sustainable Future*, Oxford University Press, Printed by Bath Press, Glasgow, 1996.
- [2] A. Bergen, T. Schmeister, L. Pitt, A. Rowe, N. Djilali, P. Wild, *J. Power Sources* 164 (2007) 624–630.
- [3] N.J. Schenk, H.C. Moll, J. Potting, R.M.J. Benders, *Energy* 32 (10) (2007) 1960–1971.
- [4] E. Troncoso, M. Newborough, *Int. J. Hydrogen Energy* 32 (13) (2007) 2253–2268.
- [5] D.C. Young, G.A. Mill, R. Wall, *Int. J. Hydrogen Energy* 32 (8) (2007) 997–1009.
- [6] E. Kasseris, Z. Samaras, D. Zafeiris, *Renewable Energy* 32 (1) (2007) 57–79.
- [7] F. Chen, N. Duic, L. Manuel Alves, M. da Graca Carvalho, *Renewable Sustainable Energy Rev.* 11 (8) (2007) 1888–1902.
- [8] E.I. Zoulias, N. Lymberopoulos, *Renewable Energy* 32 (4) (2007) 680–696.
- [9] J.D. Maclay, J. Brouwer, G.S. Samuelsen, *Int. J. Hydrogen Energy* 31 (8) (2006) 994–1009.
- [10] J.D. Maclay, J. Brouwer, G.S. Samuelsen, *J. Power Sources* 163 (2007) 916–925.
- [11] O.C. Onar, M. Uzunoglu, M.S. Alam, *J. Power Sources* 161 (1) (2006) 707–722.
- [12] S.S. Deshmukh, R.F. Boehm, *Renewable Sustainable Energy Rev.* 12 (9) (2008) 2301–2330.
- [13] R. Dufo-Lopez, J.L. Bernal-Agustin, J. Contreras, *Renewable Energy* 32 (7) (2007) 1102–1126.
- [14] A. Bilodeau, K. Agbossou, *J. Power Sources* 162 (2) (2006) 757–764.
- [15] M. Little, M. Thomson, D. Infield, *Int. J. Hydrogen Energy* 32 (10–11) (2007) 1582–1588.
- [16] R. Gazey, S.K. Salman, D.D. Aklii-D'Halluin, *J. Power Sources* 157 (2) (2006) 841–847.
- [17] T. Nakken, L. Strand, E. Frantzen, R. Rohden, P. Eide, in *European Wind Energy Conference*, 2006.
- [18] H. Bindner, Personal communication, 2007.
- [19] S. Ugursal, A.S. Fung, I.V., *Energy Buildings*, 24 (1996) 137–146.
- [20] M. Mottillo, RE-H2 Model Data, Personal communication, 2007.
- [21] B.C. Hydro, Residential power consumption data, personal communication, 2007.
- [22] A. Bergen, L. Pitt, A. Rowe, P. Wild, N. Djilali, Transient electrolyser response in a renewable–regenerative energy system, *Int. J. Hydrogen Energy*, in press, doi:10.1016/j.ijhydene.2008.10.007.
- [23] A. Bergen, Ph.D. thesis, University of Victoria, Victoria (2008).
- [24] J. Schiffer, D.U. Sauer, H. Bindner, T. Cronin, P. Lundsager, R. Kaiser, *J. Power Sources* 168 (1) (2007) 66–78.
- [25] M. Moran, H. Shapiro, *Fundamentals of Engineering Thermodynamics*, 4th ed., John Wiley and Sons, New York, 1999.